

# Initiation of antiplane shear instability under slip dependent friction

Michel Campillo<sup>1</sup>

Laboratoire de Géophysique Interne, Observatoire de Grenoble, Université Joseph Fourier  
Grenoble, France

Ioan R. Ionescu<sup>2</sup>

Laboratoire de Mathématiques, Université de Savoie, Chambéry, France

**Abstract.** We study the initiation of an unstable antiplane elastodynamic shear process under slip-weakening friction. We give an analytical expression of the slip that we interpret using an eigenvalue analysis. Considering only the part of the solution associated with positive eigenvalues, we define a “dominant part” characterized by an exponential growth with time. An explicit formula is given for the dominant part that controls the development of the instability after the application of an initial perturbation on the surface or inside the elastic body. It shows that in response to a small initial perturbation the instability will develop in a limited spectral domain. The limiting wavenumber (or reciprocal critical length) is a function of the parameters of the friction law and the elastic properties. The part of the solution associated with negative eigenvalues (the “wave part”) becomes rapidly negligible when the instability develops. We found that in the initiation phase the displacement field in the elastic body has a simple exponential dependence on the coordinate perpendicular to the fault. Using the expression of the dominant part, we estimate the duration of the initiation phase. We show the accuracy of the theoretical analysis by comparison with numerical tests computed with an independent technique. Finally, we show how the initiation phase determines the evolution toward the dynamic rupture propagation. We introduce the critical patch length in a natural way. The transition between the initiation and the propagation stages is characterized by an apparent supersonic velocity of the rupture front.

## Introduction

The investigation of friction laws on faults has been the object of considerable attention during the last decades. It emerges as a key issue for earthquake prediction. Different studies have focused on dynamic faulting and seismic cycles. We concentrate here on the short-term dynamical evolution of a simple model of a fault towards the slip instability.

Recently, *Iio* [1992, 1995] and *Ellsworth and Beroza* [1995] drew attention to the possibility of recording seismic signals associated with an initiation stage of the rupture. However, *Ohnaka* and his coworkers performed a series of experiments in which it was possible to measure directly the interdependence between the differ-

ent local variables: stress, slip and slip velocity (see *Ohnaka* [1996] for a review). These experiments show that during a slip event the friction exhibits mostly a dependence on the slip. Following these experiments, we shall consider here a slip-weakening type of friction law.

The elastic quasi-static problem with slip dependent friction was studied by *Ionescu and Paumier* [1995, 1996] where results concerning nonhomogeneous bifurcation of the static equilibrium positions were obtained. Having in mind the multiplicity of the equilibrium positions and the fact that the perfect delay criterion does not merely apply, they concluded that it is difficult to predict the new equilibrium position with a quasi-static analysis and that a dynamic analysis is required.

It was shown that the dynamical behavior of a frictional system is qualitatively different for a rigid block drifted through a spring and for one-dimensional shearing of an elastic slab *Campillo et al.*, [1996]. Therefore we shall concentrate here on the elastodynamic analysis of the friction in the antiplane case. More precisely, we focus our discussion on the initiation of the shear

<sup>1</sup> Also at Institut Universitaire de France.

<sup>2</sup> Also at Laboratoire de Modélisation et Calcul, IMAG, Grenoble, France.

process during the weakening stage to point out simple mathematical properties of its unstable evolution implied by a slip dependent friction law. We give a formula that describes the growth of the instability in a form very simple to evaluate and to interpret. The present paper is limited to this topic and does not discuss the long-term evolution of the system as done by *Cochard and Madariaga* [1994] or *Geubelle and Rice* [1995].

In the next section the antiplane elastodynamic problem with slip-weakening friction is stated. Restricting ourselves to the initiation phase, we present an explicit analytical formula of the "dominant part" of the solution, that is, the part of the solution which has an exponential time growth. This behavior is also explained through a classical stability analysis which shows that there exists an exponential time growth in a limited spectral domain (this point was already noticed by *Langer et al.* [1996] in a slightly different context). An approximative formula of the duration of the initiation phase is deduced from the expression of the dominant part. Some independant numerical tests will show the great accuracy of this analysis. Finally, using numerical tests, we discuss the transition to the crack propagation in relation to our theoretical analysis of the initiation.

**Problem Statement**

Consider the antiplane shearing of two homogeneous linear elastic half-spaces bounded by the plane  $\Gamma_f$  defined by  $y = 0$ . The half-spaces are in contact with slip dependent friction. We assume that the displacement field is 0 in directions  $Ox$  and  $Oy$  and that  $u_z$  does not depend on  $z$ . The displacement is therefore denoted simply by  $w(t, x, y)$ . The elastic media have the shear rigidity  $G$ , the density  $\rho$ , and the shear velocity  $c = \sqrt{G/\rho}$ . The nonvanishing shear stress components are  $\sigma_{zx} = \tau_x^\infty + G\partial_x w(t, x, y)$  and  $\sigma_{zy} = \tau_y^\infty + G\partial_y w(t, x, y)$ , and the normal stress on the fault plane is  $\sigma_{yy} = -S$  ( $S > 0$ ).

The equation of motion is

$$\frac{\partial^2 w}{\partial t^2}(t, x, y) = c^2 \nabla^2 w(t, x, y) \tag{1}$$

for  $t > 0$  and  $y \neq 0$ . The boundary conditions on fault plane  $\Gamma_f$  are

$$\sigma_{zy}(t, x, 0+) = \sigma_{zy}(t, x, 0-), \tag{2}$$

$$\begin{aligned} \sigma_{zy}(t, x, 0) &= \mu(x, \delta w(t, x)) S \text{sign}\left(\frac{\partial \delta w}{\partial t}(t, x)\right) \\ \partial_t \delta w(t, x) &\neq 0 \end{aligned} \tag{3}$$

$$|\sigma_{zy}(t, x, 0)| \leq \mu(\delta w(t, x)) S \quad \partial_t \delta w(t, x) = 0 \tag{4}$$

where  $\delta w(t, x) = w(t, x, 0+) - w(t, x, 0-)$  is the relative slip.

The initial conditions are denoted by  $w_0$  and  $w_1$ , that is,

$$\begin{aligned} w(0, x, y) &= w_0(x, y), \\ \frac{\partial w}{\partial t}(0, x, y) &= w_1(x, y). \end{aligned} \tag{5}$$

For simplicity, let us assume in the following that the slip  $\delta w$  and the slip rate  $\partial_t \delta w$  are positive and the friction law is homogeneous on the fault plane having the form of a piecewise linear function

$$\mu(x, \delta u) = \mu_s - \frac{\mu_s - \mu_d}{2L_c} \delta u \quad \delta u \leq 2L_c, \tag{6}$$

$$\mu(x, \delta u) = \mu_d \quad \delta u > 2L_c, \tag{7}$$

where  $\delta u$  is the relative slip,  $\mu_s$  and  $\mu_d$  ( $\mu_s > \mu_d$ ) are the static and dynamic friction coefficients, and  $L_c$  is the critical slip (Figure 1). This piecewise linear function is a reasonable approximation of the experimental observations obtained by *Ohnaka et al.* [1987].

Since our intention is to study the evolution of the elastic system near an unstable equilibrium position, we shall suppose that  $\tau_y^\infty = S\mu_s$ . We remark that taking  $w$  as a constant satisfies (1)-(4); hence  $w \equiv 0$  is an equilibrium position. Having in mind that we deal with an homogenous fault plane and with the evolution of one initial pulse, we may put (for symmetry reasons)  $w(t, x, y) = -w(t, x, -y)$ , hence we consider only one half-space  $y > 0$  in (1) and (5). With these assumptions, (2)-(4) become

$$\frac{\partial w}{\partial y}(t, x, 0+) = -\alpha_c w(t, x, 0+) \quad w(t, x, 0+) \leq L_c, \tag{8}$$

$$\frac{\partial w}{\partial y}(t, x, 0+) = -\alpha_c L_c \quad w(t, x, 0+) > L_c, \tag{9}$$

where  $\alpha_c$  is a parameter which has the dimension of a wavenumber ( $m^{-1}$ ) and which will play an important role in our further analysis. The value  $\alpha_c$  is given by

$$\alpha_c = \frac{(\mu_s - \mu_d)S}{GL_c}$$

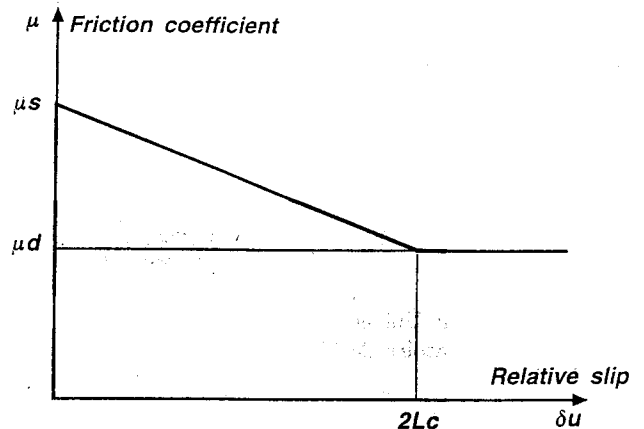


**Figure 1.** Friction coefficient  $\mu$  as a function of the relative slip  $\delta u$ .

### Instabilities in the Initiation Phase

Since the initial perturbation  $(w_0, w_1)$  of the equilibrium ( $w \equiv 0$ ) is small we have  $w(t, x, 0+) \leq L_c$  for  $t \in [0, T_c]$  for all  $x$ , where  $T_c$  is a critical time for which the slip on the fault reaches the critical value  $L_c$  at least at one point, that is,  $\sup_{x \in R} w(T_c, x, 0+) = L_c$ . Hence for a first period  $[0, T_c]$ , called in the following initiation period, we deal with a linear initial and boundary value problem (1), (5), (8). Though many methods can be used in solving this problem, we present in the appendix an elementary technique that relies mostly on the use of the Fourier transform. The formulation of the solution is adapted to the principal objective of this section: the description of the behavior of the evolution of the perturbation during the initiation phase.

As it follows from the appendix, a part of the solution will have an exponential growth with time. Hence after a while this part will completely dominate the other part which has a wave-type evolution. This is why we put  $w = w^d + w^w$ , where  $w^d$  is the "dominant part" and  $w^w$  is the "wave part." Since the expression of the wave part  $w^w$  is not relevant for our analysis of the instable growth, we give here only the simple expression of the dominant part:

$$w^d(t, x, y) = \frac{\alpha_c}{\pi} \exp(-\alpha_c y) \left\{ \int_{-\alpha_c}^{\alpha_c} \int_0^{\infty} \int_{-\infty}^{\infty} \exp(-\alpha_c s + i\alpha(x-u)) [\text{ch}(ct\sqrt{\alpha_c^2 - \alpha^2}) w_0(u, s) + \frac{\text{sh}(ct\sqrt{\alpha_c^2 - \alpha^2})}{c\sqrt{\alpha_c^2 - \alpha^2}} w_1(u, s)] dudsd\alpha \right\}. \tag{10}$$

The accuracy of the above formula in the description of the displacemet field  $w$  will be demonstrated in the section on numerical results. This expression has the advantadge of allowing a direct simple computation of the solution at a given time. It makes it possible to consider any type of initial perturbation not necessarily concentrated on the fault.

The behavior of  $w$  can also be explained through a classical stability analysis of our initial and boundary value problem. In order to do this, we consider the following eigenvalue problem (connected to (1), (5) and (8)): find a bounded eigenfunction  $v : R \times R_+ \rightarrow R$  and the eigenvalue  $\lambda$  such that

$$\nabla^2 v(x, y) = \lambda^2 v(x, y), \quad y > 0, \tag{11}$$

$$\frac{\partial v}{\partial y}(x, 0+) = -\alpha_c v(x, 0+).$$

Since we deal with unbounded domains, we have a continuous spectrum. After some algebra we get that  $\lambda^2 \leq \alpha_c^2$ , that is, a limited spectral domain, and the expression of the eigenfunctions corresponding to positive eigenvalues  $\lambda^2 \geq 0$  is

$$v_\lambda(x, y) = C_\lambda \exp(-\alpha_c y \pm ix\sqrt{\alpha_c^2 - \lambda^2}), \tag{12}$$

for  $0 \leq \lambda^2 \leq \alpha_c^2$ . Following this spectral analysis, we notice that the positive eigenvalues  $\lambda$  (i.e., for  $0 \leq \lambda^2 \leq \alpha_c^2$ ) correspond to an instable behavior (i.e., an exponential growth in time, as  $w(t, x, y) = \exp(c\lambda t)v_\lambda(x, y)$ ) and that the imaginary eigenvalues  $\lambda$  (i.e. for  $\lambda^2 < 0$ ) correspond to a stable and propagative behavior. We remark that the dominant part  $w^d$ , which corresponds to  $v_\lambda$  for  $0 \leq \lambda^2 \leq \alpha_c^2$  in the above analysis, has the same particular dependence  $\exp(-\alpha_c y)$  on the  $y$  space variable as the eigenfunction  $v_\lambda$ . Its expression indicates also that the coefficient of the exponential time growth is larger for low values of the wavenumber  $\alpha$ . In other words, the larger the characteristic length is, the larger the exponent  $c\sqrt{\alpha_c^2 - \alpha^2}$  is. This exponent is similar in this context to the Lyapunov exponent.

### Duration of the Initiation Phase

In this section we shall use the expression of dominant part  $w^d$  to find an approximative formula for  $T_c$ , the duration of the initiation phase.

Since of the evolution of the slip  $t \rightarrow w(t, x, 0+)$  is in essence described by the dominant part, we deduce that  $T_c$  satisfies  $\sup_{x \in R} w^d(T_c, x, 0+) = L_c$ . Assuming that the initial perturbation is such that the first point  $x$  of the fault for which the slip reaches the critical value  $L_c$  is  $x = 0$ , we obtain that  $T_c$  is the solution of the equation  $w^d(T_c, 0, 0+) = L_c$ .

Let us suppose that the initial perturbation is localized in a infinite strip  $[-a, a] \times [b, +\infty[$  of halfwidth  $a$  at the distance  $b \geq 0$  from the fault  $y = 0$ , that is,  $w_0(x, y) = w_1(x, y) = 0$  if  $(x, y) \notin [-a, a] \times [b, +\infty[$ . Let us introduce the following weighted average of the initial perturbation (as suggested by (10)):

$$W_0 = \frac{\alpha_c}{2a} \int_{-a}^a \int_0^{+\infty} \exp(-\alpha_c y) w_0(x, y + b) dx dy,$$

$$W_1 = \frac{\alpha_c}{2a} \int_{-a}^a \int_0^{+\infty} \exp(-\alpha_c y) w_1(x, y + b) dx dy.$$

If the initial perturbation is small and the half width is not too great, that is,  $\pi L_c / [2a(W_0 \alpha_c + W_1/c)] \gg 1$  and  $\pi / (a\alpha_c) \gg 1$ , then from (10) one can deduce the following approximative formula:

$$T_c \approx \frac{b}{c} + \frac{1}{\alpha_c} \ln \left[ \frac{\pi L_c}{2a(W_0 \alpha_c + W_1/c)} \right]. \tag{13}$$

The accuracy of this formula is verified by independent numerical computations (see the section on numerical tests). The term  $T_w = b/c$  corresponds to the travel time needed by the waves associated with the initial perturbation to reach the fault. We remark that  $T_c$  depends on the initial average  $W_0$  and  $W_1$  through a natural logarithm, hence the duration of the initiation phase has only a weak (logarithmic) dependence on the amplitude of the initial perturbation.

The above formula is valid only for a linear dependence of the friction coefficient  $\mu$  on the slip  $u$  in the weakening domain ( $u \in [0, L_c]$  in our case). If a nonlinear weakening dependence  $\mu = \mu(u)$  is considered, much slower evolution of the initiation phase can be expected in the neighborhood of the slip  $u_0$  for which  $\mu'(u_0) = 0$ .

## Numerical Tests

The theoretical development in the section on instabilities in the initiation phase indicates some strong and simple properties of the slip during the initiation phase. In particular, the essential properties of the evolution of the system are described by the simple expression (10) which we refer to as the dominant part. The aim of this paragraph is to compare these theoretical results with some numerical tests. These tests were obtained by using a numerical approach of the nonlinear problem, (1)-(5). Since the details of the numerical method are beyond the scope of the present paper, let us give here only a brief description of the numerical scheme. The second-order partial differential equation (1) is written as a first-order system involving the velocity and the two shear stress components. After splitting, an alternating direction method is used to reduce the problem to two hyperbolic systems in one space dimension for each time step. A classical finite difference scheme (Lax-Wendroff) is used in the discretization of these systems. Concerning the nonlinear boundary conditions (2)-(4), we used the integration along the characteristic lines (in the system following the  $y$  direction) to deduce an instability-capturing scheme.

In the following we will use a grid of  $1000 \times 500$  points in the  $x, y$  plane. Since we want to compare analytical and numerical results, the parameters of the computation were the same in both cases. We use the following model parameters:  $\rho = 3000 \text{ kg/m}^3$ ,  $c = 3000 \text{ m/s}$ ,  $L_c = 0.05 \text{ m}$ ,  $\mu_s = 0.8$  and  $\mu_d = 0.72$ . The normal stress is assumed to correspond to a lithostatic pressure corresponding to a depth of 5 km. The initial condition corresponds to a velocity perturbation  $w_1$  while the initial displacement perturbation  $w_0$  is 0. The initial velocity perturbation has the following distribution:

$$w_1(x, y) = A \exp\left(\frac{(x - x_0)^2}{(x - x_0)^2 - a^2} - \gamma y\right) \quad |x - x_0| < a,$$

$$w_1(x, y) = 0 \quad \text{elsewhere.} \quad (14)$$

where the half-width  $a$  is 50 m, the maximum amplitude  $A$  is 0.0001 m/s, and  $\gamma$  is equal to  $0.0872 \text{ m}^{-1}$ , which corresponds to a very rapid decay of the amplitude in the direction perpendicular to the fault. As was already noticed, the analytical expression (10) allows us to include the effect of initial conditions out of the fault plane.

A comparison between the dominant part of the analytical solution and the numerical solution is presented in Figure 2 for the beginning of the process. The slip

velocity on the fault computed by the two methods is presented as a function of space and time for times less than 0.16 s. The complete response to the initial perturbation can be seen in the results of the finite difference computation (Figure 2a). It includes the propagative part  $w^w$  introduced in our analysis of the solution behavior. The analytical dominant part  $w^d$  (see Figure

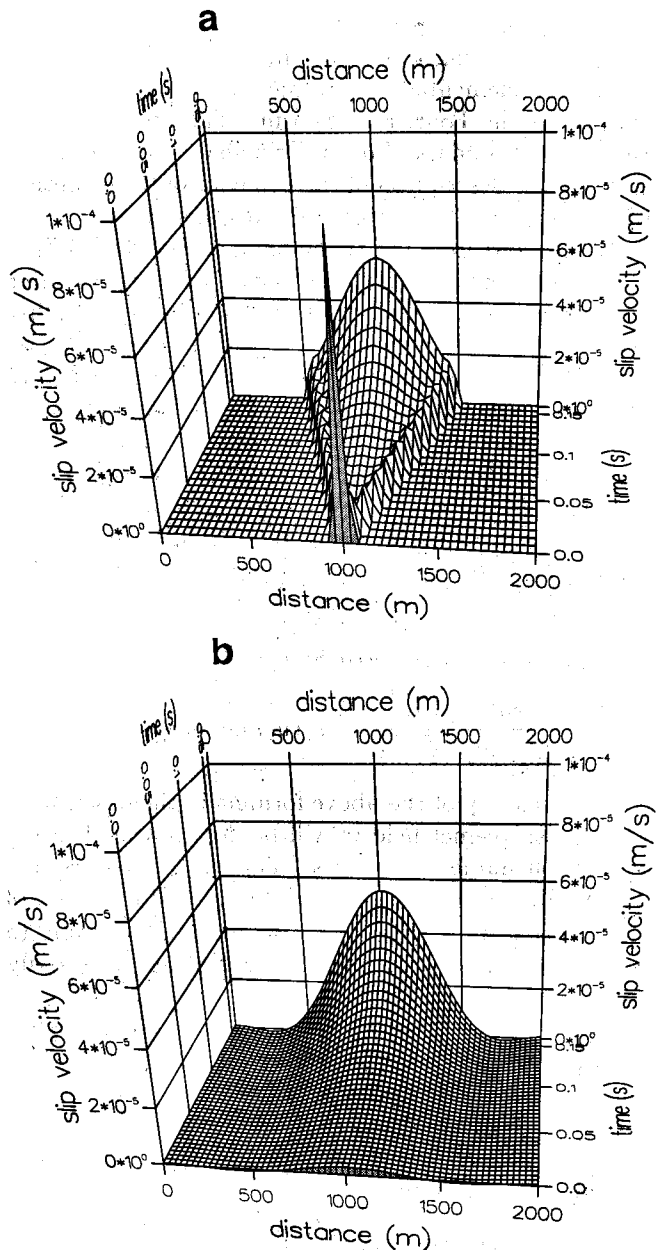


**Figure 2.** (a) Slip velocity ( $\partial_t w(t, x, 0+)$ ) on the frictional surface ( $y = 0$ ) as a function of space ( $x$ ) and time ( $t$ ) during a short window at the beginning of the initiation phase computed using a finite difference method. Note the propagation of the initial perturbation and the onset of the time exponential growth. (b) Slip velocity corresponding to the dominant part ( $\partial_t w^d(t, x, 0+)$ ) of the analytical solution given by (10) during the same short window. Note the similarity of the profile of the velocity in the center of the slipping zone at the end of this time window.

2b) comprises only the term of exponential time growth. The comparison between the two results shows that the exponential terms dominate very rapidly as indicated by the fact that the two solutions agree very well in amplitude at the end of the time window.

The use of the expression of the dominant part (Figure 2b) leads to a solution in which the perturbation has been severely smoothed by the finite wavenumber integration of (10). The hyperbolic terms are not taken into account in the dominant part, so the propagation of the perturbation is not represented, and therefore the development of the slip does not comply with causality. This is not a serious problem since the propagative terms are rapidly negligible and the shape of the slip distribution is almost perfectly described by the dominant part. This is illustrated in Figure 3. In this case the computation is performed up to the time when the critical slip is reached. The slip velocity computed using the finite difference technique is plotted in Figure 3a. The value of the slip velocity at the critical time is 4 orders of magnitude larger than the initial perturbation. A plot of the dominant part of the solution is visually identical to the one shown in Figure 3a. We have therefore plotted the arithmetic difference between the two solutions in Figure 3b. It indicates that the maximum values reached by the exponentially growing slip velocity differ by a few percent in the two types of computation. This high precision illustrates the validity of our analysis and the great accuracy of (10) describing the growth of the instability.

Concerning the evaluation of the duration of the initiation phase, (13) gives  $T_c = 0.52223$  s and both the finite difference method and the analytical expression of the dominant part, (10), indicate that the critical slip is reached after  $T_c = 0.560$  s. We remark that the approximate formula (13) gives a rather good estimate of  $T_c$  in this case.

### Characteristics of the Initiation Phase

An important and somehow unexpected property revealed by the theoretical analysis is the  $y$  dependence of the dominant part during the period when the friction is linearly decreasing. The very simple exponential decay of (10) can be visualized in the finite difference results by plotting the natural logarithm of the slip velocity at a fixed time as done in Figure 4. Here the slip velocity is plotted at the time  $T_c$  when the critical slip is reached. In the causality domain, that is, in the domain reached by the waves, the decay is almost perfectly exponential with an argument independent of the position as indicated by the straight line on the logarithmic plot. A linear regression indicates that the argument is precisely  $\alpha_c$  as expected from the theory. This accuracy is remarkable if we consider that the range of evolution of the slip rate in this numerical experiment is approximately 6 orders of magnitude.

The corroboration of the analytical solution with the numerical results shows the possibility of using the expression of the dominant part to describe the properties of the initiation phase in our model. An advantage of the (10) is the explicit delineation of the part played by the different parameters. The expression indicates that the strongest rate of growth corresponds to low

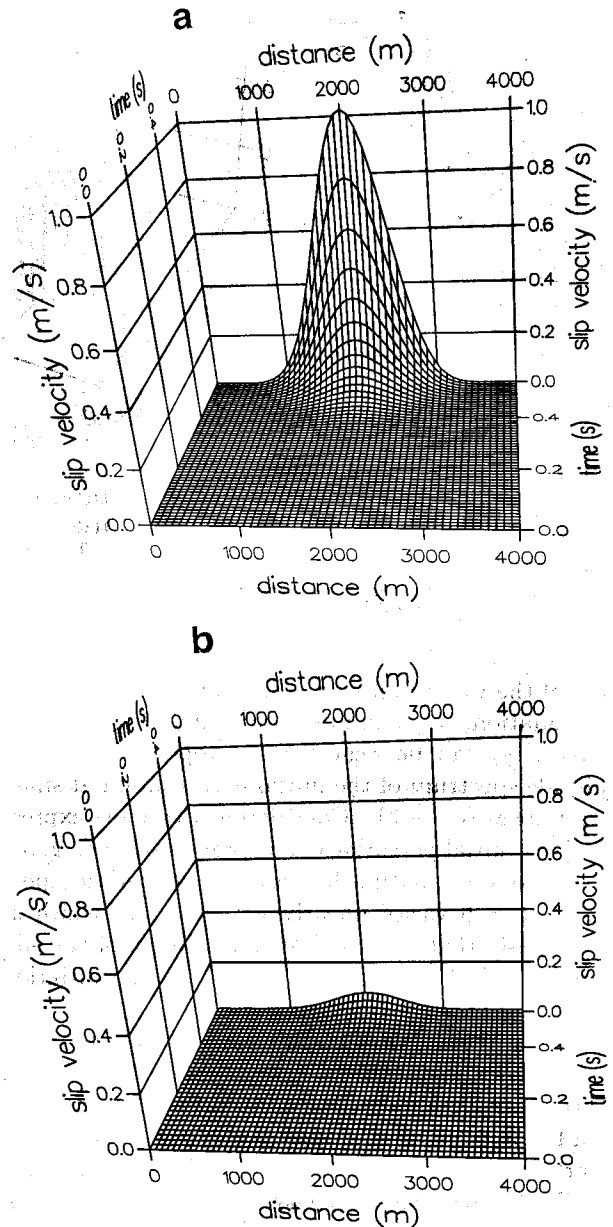


**Figure 3.** (a) Slip velocity ( $\partial_t w(t, x, 0+)$ ) on the frictional surface ( $y = 0$ ) as a function of space ( $x$ ) and time ( $t$ ) during the entire initiation phase ( $0 < t < T_c$ ) computed using a finite difference method. Note that the slip velocity at the beginning of the initiation phase, plotted in Figure 2 a, is not visible at this scale. (b) Difference ( $\partial_t w(t, x, 0+) - \partial_t w^d(t, x, 0+)$ ) between the slip velocity given by the finite difference method plotted in Figure 3 a and the slip velocity computed using only the expression of the dominant part of the analytical solution given by (10).

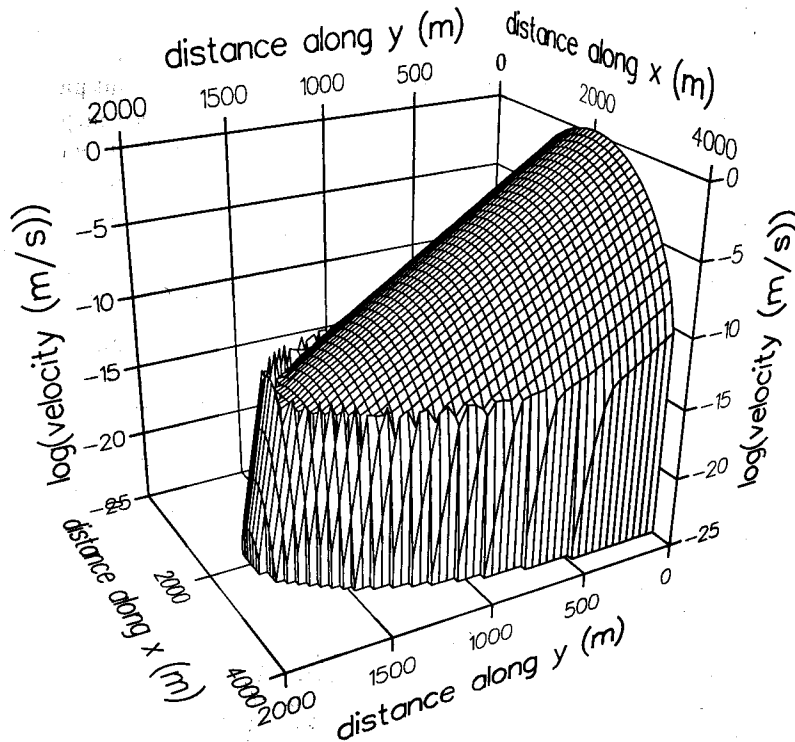


**Figure 4.** Distribution of the natural logarithm of the velocity ( $\ln(\partial_t w(T_c, x, y))$ ) in the elastic body as a function of space variables  $x$  and  $y$  at the end of the initiation phase ( $t = T_c$ ). Computation is done using the finite difference method. The parameters of the model are the same as in Figures 2 and 3. Note the perfect exponential behavior of the velocity with respect to the  $y$  variable.

values of the wavenumber  $\alpha$ . Therefore, as a first-order approximation, the maximum amplitude of the slip (or slip velocity) can be regarded as proportional to the amplitude spectrum of the initial perturbation at small wavenumbers ( $\alpha \rightarrow 0$ ). Considering the same expression of the initial perturbation as previously (i.e., given by (14)), we note that in this case the value of the spectrum at  $\alpha = 0$  varies linearly with the half width  $a$ . This suggests that the maximum amplitude of the slip (or slip velocity) at a given time during the initiation phase would be almost proportional to  $a$ .

To check the validity of this proposition, we computed the maximum slip velocity 0.48 s after the initial perturbation for half widths of 10, 20, 50, 100, 300 and 600 m keeping all other parameters of the computation similar to the ones used in the section on numerical tests. The value of slip velocity reached for  $a = 100$  m (0.215 m/s) is almost twice the one reached with  $a = 50$  m (0.108 m/s). We verified that a perfect linearity is obtained for half width less than 50 m. However the value obtained for  $a = 300$  m (0.624 m/s) is less than 6 times the one obtained for  $a = 50$  m. This departure from linearity is even stronger for  $a = 600$  m with a maximum value of 1.12 m/s. This behavior is well explained by considering both the finite spectral domain on which is defined the dominant part (10) and the amplitude spectrum of the initial perturbation as shown in Figure 5. Figure 5 indicates that the spectrum of

the perturbation is almost flat in the range  $[0, \alpha_c]$  for  $a$  smaller than 100 m. In this case an almost perfect linearity with  $a$  is expected. For values of  $a$  larger than 100 m, the shape of the spectrum makes our first-order ap-

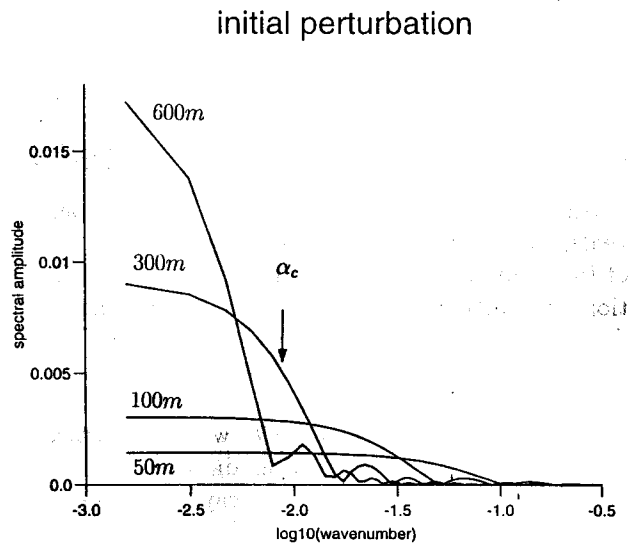


**Figure 5.** Amplitude spectra of the distribution of the initial slip rate perturbation, as a function of the wavenumber, for half widths of 50 m, 100 m, 300 m, and 600 m as indicated. The arrow indicates the value of  $\alpha_c$ . The domain of integration of the dominant part is limited to  $|\alpha| < \alpha_c$ .

proximation inaccurate, and the integration on  $\alpha$  has to be performed, leading to the departure from the simple linear behavior. This simple example shows the potential importance of the shape of the perturbation in the development of the instability in spite of the prominent part played by the small wavenumber limit in (10). This discussion corresponds to particular initial conditions, but similar conclusions could be reached for any other shapes.

## Initiation and Crack Propagation

As we mentioned in the introduction, we use a slip dependent friction law following the experimental results of *Ohnaka* [1996]. In these experiments both initiation and crack propagation were investigated. The evolution of the system in the initiation phase that we study theoretically here is fundamental in understanding how the dynamic crack propagation develops. Rapidly after the initial perturbation, the dominant exponential part governs the time and space evolution of the slip until the critical slip  $L_c$  has been reached at some point of the surface. Since a part of the slipping surface already reached the critical slip while other parts are still at rest or in the exponential growth domain, the state of the system becomes complex. This stage cannot be simply described analytically, but the finite difference solution will help in showing the main characteristics of the beginning of the dynamic crack propagation. A numerical experiment in which the system evolves toward the dynamic crack propagation is presented in Figure 6. All the parameters are equal to the ones used in Figures 2 and 3 except the total duration that is 1 s in this case. In the problem studied here the crack propagation begins in the center after the slip reaches its critical value  $L_c$ . The lapse time from the initial perturbation  $T_c$  depends on the amplitude and the shape of the initial perturbation and on the parameter  $\alpha_c$ . In the case presented here, the lapse time is somehow arbitrary since we chose the initial perturbation for practical computational purposes only.

For long times (time longer than 0.60 s in our experiment), the slip velocity behaves qualitatively as it would be in the case of a propagating crack. Indeed, in our problem there is no singularity but a concentration of the slip velocity. In the propagating steady state the width of the concentration is governed by the parameters of the friction law. At a given point on the fault the slip velocity increases until the slip reaches its critical value  $L_c$ . A similar behavior was described by *Ida* [1972] for steady propagation of a cohesive crack. *Gariel and Campillo* [1989] showed how the shape of the slip velocity concentration affects the high-frequency radiation from a fault.

Also, for long times the peak of the slip velocity (the seismic rupture front) is delayed with respect to the wave emitted at the initial perturbation (shown as straight lines on Figure 6), but it tends to propagate at

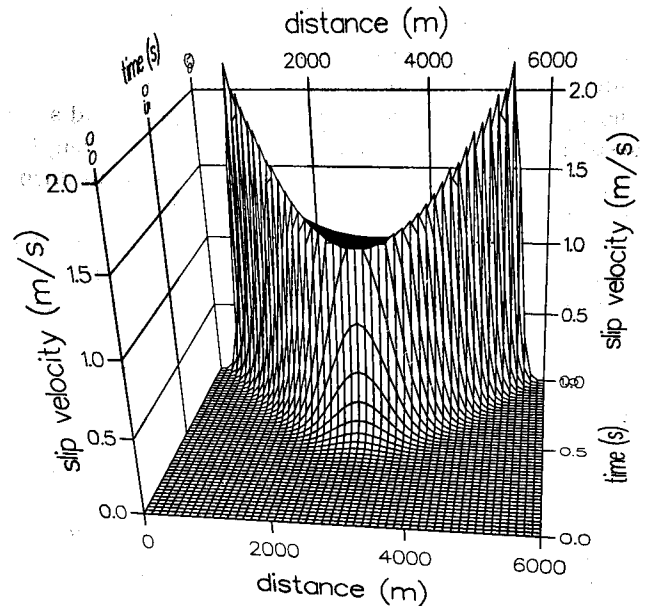


**Figure 6.** Slip velocity ( $\partial_t w(t, x, 0+)$ ) on the frictional surface ( $y = 0$ ) as a function of space ( $x$ ) and time ( $t$ ) computed using a finite difference method during the initiation stage and the transition to the steady state propagation. The straight lines indicate the arrival time of the shear waves emitted from the center of the initial perturbation. Note the supersonic velocity of the slip velocity concentration immediately after the initiation phase. Then the rupture front velocity tends to the shear wave velocity.

the shear wave velocity. A similar delay between propagating waves and the rupture front has been observed in *Ohnaka's* [1996] [1996] experiments.

The importance of the initiation phase for the further development of the rupture cannot be reduced to the existence of the delay that we just described. As a matter of fact, between the steady state propagation of the rupture discussed just above and the initiation phase, a transition phase exists. This transition phase corresponds to the time window 0.5 – 0.6 s in Figure 6. The state of the system at this stage is completely determined by the properties of the initiation phase. A striking feature is the extremely high apparent velocity (supersonic) of the rupture front when the rupture propagation begins. This phenomenon occurs because the critical slip is reached almost simultaneously on a patch of finite length. This length is, indeed, related to the shape of the slip distribution at the end of the initiation phase. It was already shown that the patch on which the exponential growth develops has a minimum width because of the limited wavenumber domain of the dominant part. According to (10), the characteristic half width of the slipping zone at the end of the initiation phase must be greater than a critical length  $a_c$  given by

$$a_c = \frac{\pi}{\alpha_c} = \frac{\pi G L_c}{(\mu_s - \mu_d) S}$$

This expression of the critical length has a form similar to the one proposed by *Dietrich* [1986, 1992] in a quite different context for a state dependent friction law and using results from the analysis of spring and slider systems. We have shown here that the critical length is implied by the unstable evolution of the system during the initiation phase.

On a seismological point of view the rupture velocity is an important parameter since the high frequency wave radiation is governed by the slip velocity concentration and its kinematics *Madariaga* [1977]. Our results show that, at the beginning of its propagation, the rupture front is supersonic. A locally supershear rupture velocity is an important feature for strong motion seismology since very high velocities would enhance both the high frequency radiation and the directivity function (see, e.g. *Madariaga* [1977] or *Campillo* [1983]).

## Conclusions

The initiation of an unstable antiplane elastodynamic shear process under slip-weakening friction was studied. An analytical expression of the slip has been given that was interpreted using an eigenvalue analysis. Considering only the part of the solution associated with positive eigenvalues, a dominant part characterized by an exponential growth with time is introduced. An explicit formula was given for the dominant part for any initial perturbation on the fault or in the elastic body. This formula shows that in response to an initial small perturbation the instability will develop in a limited spectral domain. The limiting wavenumber (or reciprocal critical length) is given in terms of the parameters of the friction law and the elastic properties. The part of the solution associated with negative eigenvalues (the wave part) becomes rapidly negligible when the instability develops. By comparing the theoretical results with numerical tests computed with an independent technique, the accuracy of our analysis was demonstrated. At the end of the initiation phase the displacement and stress fields in the elastic body have a simple exponential dependence  $\exp(-\alpha_c y)$  on the coordinate perpendicular to the fault. The duration of the initiation phase can be estimated by a simple formula. Finally we showed how the initiation phase determines the evolution toward the dynamic rupture propagation. The critical patch length appears to be a natural consequence of the evolution of the slip during the initiation phase. The rupture front exhibits a supersonic velocity during the transition between the initiation and the propagation stages.

## Appendix

The aim of this section is to find an analytical form of  $w$ , the solution of (1), (5) and (8), that exhibits explicitly the dominant part (i.e., the part of the solution

which has an exponential time growth). Although many methods can be used in solving this linear initial and boundary value problem, we present here an elementary technique which is well adapted to our objective.

We consider the following problem: find  $w : R_+ \times R \times R_+ \rightarrow R$  solution of

$$\frac{\partial^2 w}{\partial t^2}(t, x, y) = c^2 \nabla^2 w(t, x, y) \quad y > 0,$$

$$\frac{\partial w}{\partial y}(t, x, 0+) = -\alpha_c w(t, x, 0+),$$

$$w(0, x, y) = w_0(x, y),$$

$$\frac{\partial w}{\partial t}(0, x, y) = w_1(x, y).$$

In order to reduce our problem to the wave equation on the half-plane with homogeneous boundary conditions let us introduce the auxiliary function  $\Psi$ :

$$\Psi(t, x, y) = \frac{\partial w}{\partial y}(t, x, y) + \alpha_c w(t, x, y) \quad y > 0,$$

which satisfies

$$\frac{\partial^2 \Psi}{\partial t^2}(t, x, y) = c^2 \nabla^2 \Psi(t, x, y) \quad y > 0,$$

$$\Psi(t, x, 0+) = 0,$$

$$\Psi(0, x, y) = \frac{\partial w_0}{\partial y}(x, y) + \alpha_c w_0(x, y),$$

$$\frac{\partial \Psi}{\partial t}(0, x, y) = \frac{\partial w_1}{\partial y}(x, y) + \alpha_c w_1(x, y).$$

Using the usual Fourier transform we get:

$$\begin{aligned} \Psi(t, x, y) = & \frac{1}{4\pi^2} \int_{-\infty}^{\infty} \int_0^{\infty} \int_{-\infty}^{\infty} \int_0^{\infty} \exp(i\alpha(x-u)) \\ & [\cos(ct\sqrt{\alpha^2 + \beta^2})w_0(u, s) + \frac{\sin(ct\sqrt{\alpha^2 + \beta^2})}{c\sqrt{\alpha^2 + \beta^2}}w_1(u, s)] \\ & (\alpha_c \sin(\beta s) - \beta \cos(\beta s)) \sin(\beta y) ds du d\beta d\alpha. \end{aligned} \quad (15)$$

Let us introduce now the auxiliary function  $\Phi$

$$\Phi(t, x) = 2\alpha_c \int_0^{\infty} \exp(-\alpha_c s) w(t, x, s) ds. \quad (16)$$

After some algebra we find that  $w$  can be written as

$$\begin{aligned} w(t, x, y) = & [\Phi(t, x) - \int_0^{\infty} \exp(-\alpha_c s) \Psi(t, x, s) ds] \\ & \exp(-\alpha_c y) + \int_0^y \exp(-\alpha_c(y-s)) \Psi(t, x, s) ds, \end{aligned} \quad (17)$$

that is, we can easily obtain  $w$  if we have  $\Phi$ .

From (1), (5) and (16) we deduce that  $\Phi$  is the solution of the following standard wave equation in one space dimension:



$$\frac{\partial^2 \Phi}{\partial t^2}(t, x) = c^2[\alpha_c^2 \Phi(t, x) + \frac{\partial^2 \Phi}{\partial x^2}(t, x)]$$

$$\Phi(0, x) = 2\alpha_c \int_0^\infty \exp(-\alpha_c s) w_0(x, s) ds,$$

$$\frac{\partial \Phi}{\partial t}(0, x) = 2\alpha_c \int_0^\infty \exp(-\alpha_c s) w_1(x, s) ds.$$

Using the Fourier transform, we obtain the following expression of  $\Phi$ :

$$\begin{aligned} \Phi(t, x) = \frac{\alpha_c}{\pi} \left\{ \int_{-\infty}^\infty \int_0^\infty \int_{-\infty}^\infty \exp(-\alpha_c s + i\alpha(x-u)) \right. \\ \left. [\text{ch}(ct\sqrt{\alpha_c^2 - \alpha^2}) w_0(u, s) + \right. \\ \left. \frac{\text{sh}(ct\sqrt{\alpha_c^2 - \alpha^2})}{c\sqrt{\alpha_c^2 - \alpha^2}} w_1(u, s)] dudsd\alpha \right\}. \end{aligned} \quad (18)$$

We remark that for wavenumber  $\alpha \in [-\alpha_c, \alpha_c]$  the function  $\Phi$  has an exponential growth with respect to the time variable, hence the dominant part, denoted  $\Phi^d$ , of  $\Phi$  is given by :

$$\begin{aligned} \Phi^d(t, x) = \frac{\alpha_c}{\pi} \left\{ \int_{-\alpha_c}^{\alpha_c} \int_0^\infty \int_{-\infty}^\infty \exp(-\alpha_c s + i\alpha(x-u)) \right. \\ \left. [\text{ch}(ct\sqrt{\alpha_c^2 - \alpha^2}) w_0(u, s) + \right. \\ \left. \frac{\text{sh}(ct\sqrt{\alpha_c^2 - \alpha^2})}{c\sqrt{\alpha_c^2 - \alpha^2}} w_1(u, s)] dudsd\alpha \right\} \end{aligned} \quad (19)$$

One can now put (15) and (18) into (17) to deduce the analytical form of  $w$ . We remark that we have an exponential growth in time only in  $\Phi$ , hence the dominant part, denoted  $w^d$ , of  $w$  is given by

$$w^d(t, x, y) = \exp(-\alpha_c y) \Phi^d(t, x),$$

where  $\Phi^d$  is given by (19).

**Acknowledgments.** We thank R.J. Archuleta and L. Knopoff for their careful review of the original manuscript. We acknowledge financial support from program PNRN of INSU/CNRS and from project SIGMAS of IMAG (Université Joseph Fourier). Numerical simulations were performed at the "Centre de Calcul Intensif de l'Observatoire de Grenoble".

## References

Campillo, M., Numerical evaluation of near field, high frequency radiation from quasi-dynamic circular faults, *Bull. Seismol. Soc. Am.* 73, 723-734, 1983.  
 Campillo, M., I.R. Ionescu, J.C. Paumier, and Y. Renard, On the dynamic sliding with friction of a rigid block and an infinite elastic slab, *Phys. Earth. Planet. Inter.*, 96,15-23 1996.

Cochard, A., and R. Madariaga, Dynamic faulting under rate dependent friction, *Pure Appl. Geophys.*, 142, 419-445, 1994.  
 Dietrich, J.H., A model for the nucleation of earthquake slip, in *Earthquake source mechanics, Geophys. Monogr. Ser.*, vol 37, edited by S. Das, J. Boatwright and C.H. Sholz, pp 37-47, AGU, Washington, D.C., 1986.  
 Dietrich, J.H., Earthquake nucleation on faults with rate- and state-dependent strength, *Tectonophysics*, 211, 115-134, 1992.  
 Ellsworth, W.L., and G.C. Beroza, Seismic evidence for an earthquake nucleation phase, *Science*, 268, 851-855, 1995.  
 Gariel, J.C. and M. Campillo, The influence of the source on the high-frequency behavior of the near field acceleration spectrum: A numerical study, *Geophys. Res. Lett.*, 16 (4), 279-282, 1989.  
 Geubelle, P., and J.R. Rice, A spectral method for 3D elastodynamic fracture problem, *J. Mech. Phys. Solids*, 43, 1791-1824, 1995.  
 Ida, Y., Cohesive force across the tip of a longitudinal-shear crack and Griffith's specific surface energy, *J. Geophys. Res.*, 77, 3796-3805, 1972.  
 Iio, Y., Slow initial phase of the P-wave velocity pulse generated by microearthquakes, *Geophys. Res. Lett.*, 19(5), 477-480, 1992.  
 Iio, Y., Observations of the slow initial phase generated by microearthquakes: Implications for earthquake nucleation and propagation, *J. Geophys. Res.*, 100, 15333-15349, 1995.  
 Ionescu, I.R., and J.-C. Paumier, Slip displacement dependent friction in quasi-static elasticity, in *Contact Mechanics*, edited by M. Raous et al., pp. 119-127, Plenum, New York, 1995.  
 Ionescu, I.R., and J.-C. Paumier, On the contact problem with slip dependent friction in elastostatics, *Int. J. Eng. Sci.*, 34(4), 471-491, 1996.  
 Langer, J.S., J.M. Carlson, R.M. Myers, and E. Shaw, Slip complexity in dynamic models of earthquake faults, *Proc. Natl. Acad. Sci. U.S.A.*, 93, 3825-3829, 1996.  
 Madariaga, R., High-frequency radiation from crack (stress drop) models of earthquake faulting, *Geophys. J. R. Astron. Soc.*, 51, 625-651, 1977.  
 Ohnaka, M., Nonuniformity of the constitutive law parameters for shear rupture and quasistatic nucleation to dynamic rupture: A physical model of earthquake generation model, paper presented at Earthquake Prediction: The Scientific Challenge, U.S. Acad. of Sci., Irvine, Calif., 1996.  
 Ohnaka, M., Y. Kuwahara, and K. Yamamoto, Constitutive relations between dynamic physical parameters near a tip of the propagation slip during stick-slip shear failure, *Tectonophysics*, 144, 109-125, 1987.

Michel Campillo, Laboratoire de Géophysique Interne, Observatoire de Grenoble, Université Joseph Fourier, BP 53X, 38041 Grenoble Cedex, France. (e-mail: Michel.Campillo@ujf-grenoble.fr)

Ioan R. Ionescu, Laboratoire de Mathématiques, Université de Savoie, 73376 Le Bourget-du-Lac Cedex, France. (e-mail: ionescu@univ-savoie.fr)

(Received August 6, 1996; revised February 5, 1997; accepted May 19, 1997.)